HHS Public Access

Author manuscript

Biochem Biophys Res Commun. Author manuscript; available in PMC 2023 December 03.

Published in final edited form as:

Biochem Biophys Res Commun. 2022 December 03; 632: 173–180. doi:10.1016/j.bbrc.2022.09.084.

Fluid shear stress enhances proliferation of breast cancer cells via downregulation of the c-subunit of the F_1F_O ATP synthase

Han-A Park[a,*], **Spenser R. Brown**[b], **Joseph Jansen**[a], **Tracie Dunn**[a], **Madison Scott**[a], **Nelli Mnatsakanyan**[c,d], **Elizabeth A. Jonas**[c], **Yonghyun Kim**[b]

[a]Department of Human Nutrition and Hospitality Management, College of Human Environmental Sciences, The University of Alabama, Tuscaloosa, AL, 35487, USA

[b]Department of Chemical and Biological Engineering, College of Engineering, The University of Alabama, Tuscaloosa, AL, 35487, USA

[c]Department of Internal Medicine, Section of Endocrinology, Yale University, New Haven, CT, 06511, USA

[d]Department of Cellular and Molecular Physiology, The Pennsylvania State University College of Medicine, Hershey, PA, 17033, USA

Abstract

The presence of circulating cancer cells in the bloodstream is positively correlated with metastasis. We hypothesize that fluid shear stress (FSS) occurring during circulation alters mitochondrial function, enhancing metastatic behaviors of cancer cells. MCF7 and MDA-MB-231 human breast cancer cells subjected to FSS exponentially increased proliferation. Notably, FSS-treated cells consumed more oxygen but were resistant to uncoupler-mediated ATP loss. We found that exposure to FSS downregulated the F_1F_O ATP synthase c-subunit and overexpression of the c-subunit arrested cancer cell migration. Approaches that regulate c-subunit abundance may reduce the likelihood of breast cancer metastasis.

Keywords

Mitochondria; Breast cancer; Fluid shear stress; F_1F_O ATP synthase

1. Introduction

Circulating tumor cells (CTCs) are cancer cells that have detached from the primary tumor site and are transported via the bloodstream. Although the total number of detectable CTCs in blood samples is low [1], a small number of viable CTCs traveling through the circulation is sufficient to promote metastatic tumor development. Moreover, up to 90% of cancer mortality is due to cancer metastasis [2]. In breast cancer, the number of CTCs is inversely

*Corresponding author. Department of Human Nutrition and Hospitality Management, College of Human Environmental Sciences, The University of Alabama, PO Box 870311, Tuscaloosa, AL, 35487, USA., hpark36@ches.ua.edu (H.-A. Park).

Declaration of competing interest

The authors declare no conflict of interest.

correlated to progression-free intervals and overall survival rate [1,3,4]. The presence of CTCs is also associated with breast cancer recurrence [5,6]. Researchers have shown that CTCs exhibit strong cancer stem cell progenitor phenotypes, chemoresistance, and anti-apoptotic characteristics, all of which contribute to metastatic potential [7–9]. Despite their significance in breast cancer progression, cellular mechanisms of CTC-mediated breast cancer metastasis and the molecular targets responsible for CTC survival have seldom been investigated.

The F_1F_O ATP synthase is a multiprotein complex that produces ATP using the proton gradient generated by the electron transport chain. Although the central role of F_1F_O ATP synthase is to govern mitochondrial energy metabolism, an increasing number of studies have demonstrated the unique features of F_1F_O ATP synthase subunits. Notable among these is the c-subunit, a key subunit embedded in the mitochondrial inner membrane that forms a transmembrane ring structure and has been shown under physiological and pathological conditions to conduct ions as a non-selective leak channel. The c-subunit has been suggested to form the mitochondrial permeability transition pore (mPTP) and the large conductance mitochondrial death channel [10–15]. Our research group and others have reported that depletion of the c-subunit prevents large channel activity, loss of mitochondrial inner membrane potential, and cell death upon stimulation of permeability transition [11,12].

In this study, we employed fluid shear stress (FSS), the biophysical force created by the dynamic circulatory environment, to mimic the biophysical characteristics to which CTCs are exposed. We found that the proliferation of MCF7 and MDA-MB-231 breast cancer cells subjected to FSS increased relative to the static control. Furthermore, FSS treatment resulted in mitochondrial remodeling and altered mitochondria-dependent energy metabolism. Notably, FSS decreased c-subunit protein levels in breast cancer cells. Moreover, overexpression of the c-subunit slowed the migration of MCF7 and MDA-MB-231 cells, indicating that the c-subunit may be an important therapeutic target to prevent CTC-mediated metastasis.

2. Materials and methods

2.1. Breast cancer cell culture

Human breast cancer cell line MCF7 and MDA-MB-231 (ATCC, Manassas, VA) were cultured in Dulbecco's Modified Eagle's Medium (DMEM) (Thermo Fisher Scientific, Waltham, MA) supplemented with 10% fetal bovine serum (FBS) and 1X penicillin-streptomycin as previously described [7]. Cells were grown in a humidified atmosphere of 95% air and 5% CO_2 at 37 °C. Detailed information about cell culture conditions for individual studies are described in their respective figure legends.

2.2. Fluid shear stress (FSS) exposure

8×10^6 cells were resuspended in 4 mL PBS and loaded into a 5 mL plastic syringe. A Luer lock fitting was attached to the end of the syringe and connected to a polyetherether ketone (PEEK) tubing (inner diameter, 125 μm) that fed into a 50 mL centrifuge tube. The syringe plunger was pushed using a syringe pump to flow the cell solution at flowrates coresponding

to wall shear stresses of 5, 20, or 60 dyn/cm^2. The syringe was regularly agitated to maintain the suspension of the cells. After shear, cells were centrifuged at 300 rcf for 3 min and resuspended in DMEM/10% FBS.

2.3. Calcein staining

Cells were seeded onto 35 mm plates at a low density (0.1×10^6 cells/35 mm plate). After 1, 2, 3, 5, and 7 d incubation, cells were treated with Calcein-AM (Thermo Fisher Scientific, Waltham, MA). Calcein-AM (25 nM) and 1 μg/mL Hoechst were added to the culture medium for 30 min incubation at 37 °C in the dark. Micrographs were taken using a Zeiss Axiovert A1 (Zeiss, Oberkochen, Germany).

2.4. Oxygen consumption assay

The level of cellular oxygen consumption was measured by applying a fluorescence-based probe, MitoXpress Xtra (Agilent) as per manufacturer's protocol. In brief, MitoXpress Xtra (10 μl) was added to cells (90 μl media) grown in 96-well plate. Immediately after treatment, all wells were sealed with 100 μl mineral oil. Antimycin (1 μM), an inhibitor of the Complex III, was used as a negative control.

2.5. Measurement of ATP production

Cells were additionally treated 24 h after FSS with or without 10 μM FCCP. Cellular ATP production was measured using the ATPlite™ Luminescence Assay System (PerkinElmer, Waltham, MA, USA) as previously described [16]. Briefly, the plates were washed with sterile PBS and cells were lysed on the shaker for 5 min. Cells were incubated with the substrate (luciferin) on the shaker for 10 min. The reaction between ATP, luciferase and luciferin produced bioluminescence. ATP-induced luminescence was measured using a fluorescence microplate reader (CLARIOstar, BMG Labtech).

2.6. 2′,7′-dichlorodihydrofluorescein diacetate (H_2DCFDA) staining

Cells were treated with 10 μM of DCF (Thermo Fisher Scientific, Waltham, MA) solution prepared in a light protected vessel, then incubated for 30 min at 37 °C in the dark [17], and then processed as previously described [18]. After incubation, cells were carefully washed with pre-warmed HBSS. Intracellular fluorescence was measured using a fluorescence microplate reader (CLARIOstar, BMG Labtech) at excitation and emission wavelengths of 483 nm and 530 nm, respectively.

2.7. MitoSOX staining

Production of mitochondrial superoxide was analyzed using MitoSOX Red (Thermo Fisher Scientific, Waltham, MA) [18]. The MitoSOX Red is oxidized by superoxide in the mitochondria, emitting red fluorescence. After treatment of cells as described in relevant figure legends, 1.25 μM of MitoSOX was added to the cell culture medium. Cultures were incubated for 30 min at 37 °C and washed twice with warm HBSS. Micrographs were taken using a Zeiss Axiovert A1 and fluorescence intensity was analyzed using AxioVision 4.9.

2.8. Tetramethylrhodamine methyl ester (TMRM) assay

Cells were collected from 6-well plates 24 h after FSS and resuspended in TMRM (Thermo Fisher Scientific, Waltham, MA) in 1*X* PBS at concentrations ranging from 0 to 1 μM. Per the manufacturer's protocol, the cells were incubated in the TMRM solution for 30 min at 37 °C (5% CO_2), centrifuged at 300×g for 3 min, resuspended in PBS and analyzed via flow cytometry (BD Accuri C6, BD Biosciences, Franklin Lakes, NJ, USA). Each sample was analyzed in triplicate, and the data were analyzed using Flowjo (v10).

2.9. Lactate assay

The cellular lactate level was measured using an L-lactate assay kit (Eton Bioscience, Charlestown, MA) according to the manufacturer's recommendations. Briefly, an L-lactate assay solution was added to cells grown in 96-well plates. After 30 min incubation at 37 °C, the reaction was stopped by adding 0.5 M acetic acid, and the absorbance was measured at 490 nm using a microplate reader (CLARIOstar, BMG Labtech).

2.10. qRT-PCR

The NCBI gene database was used to select the primer sequences as shown:

ATPG1 forward: GTG AGT CTG TCA CCT TGA GCC, reverse: CTG CAC TCC TAC TAC CCT GCA A; *ATPG2* forward: GTC AAG AGC ACC TCA CAG C, reverse: TCT GTC AGT ATC TCC GGT CGT; *ATPG3* forward: TTA ATG GGG CCC AGA ATG GTG, reverse: CCA GCC ACT CCT ACT GTT GC; *ATP5A1* forward: TGG AGC CCA GCA AGA TTA CA; reverse: TGA TAG TGC CCA ACA AGG CT; *ATPAF2* forward: TTG AAG AAA CTG GGC GTG TC, reverse: CTG CTT GAA CAT TCC TCA GCC; *ATP5B* forward: CGC AAA CAT CTC CTT CGC CA, reverse: AGT CCC TCA TCA AAC TGG ACG; *ATPAF1* forward: TAT GTG CTC TGC CAA GAA GGG, reverse: AAG TGG AGT TCA GTA CCT GTC C; *ATP-BL* forward: ACC TCA CAT CTG ACC CTG GA, reverse: AAG CTT CCC TTC TTG GCC TC; housekeeping gene *ACTB* forward: GCC CTG GACT TCG AGC AAG AGA, reverse: ATG GTG ATG ACC TGG CCG TCA.

RNA was isolated using GeneJet RNA Purification kit (Thermo Fisher Scientific, Pittsburg, PA, USA). The manufacturer's protocol was followed for mammalian cultured cells. RNA was quantified using NanoDrop 2000 according to the manufacturer's protocol (Thermo Scientific, Wilmington, DE, USA). Complementary DNA (cDNA) was synthesized using qScript cDNA SuperMix (Quanta Biosciences, Gaithersburg, MD, USA) and Mastercycler Nexus Gradient (Eppendorf, Hauppauge, NY, USA) according to the manufacturer's protocol. Applied Biosystems PowerUp SYBR Green Master Mix was used according to the manufacturer's protocol for real-time PCR (Fisher Scientific, Hampton, NH, USA). StepOnePlus Real-Time PCR System was used for qRT-PCR (Thermo Fisher Scientific). StepOne Software (v2.3) was used for data analysis.

2.11. Immunoblotting

24 h after FSS exposure, cells were scraped from the plate and lysed in 1X RIPA buffer (Cell signaling Technology, Danvers, MA), and protein concentrations were determined using BCA protein reagents (Thermo Scientific, Rockford, IL). Samples (30–70 μg protein/lane)

were separated on a 4–12% SDS-polyacrylamide gel (Bio-Rad, Hercules, CA) and probed with anti-c-subunit (Abcam, Cambridge, UK, 1:100), anti-α-subunit (Abcam 1:1000), anti-β-subunit (Abcam 1:1000), and anti-β-actin (Sigma, St. Louis, MO, 1:2000) antibodies. Scanned images were analyzed using ImageJ software (National Institutes of Health, Bethesda, MD).

2.12. Scratch assay

Immediately after FSS exposure, cells were seeded on plates (0.8×10^6 cells/35 mm plate) and grown in an incubator (5% CO2 at 37 °C). After 24 h incubation, a straight line was scratched onto the plate using a sterile 10 μl pipette tip. Scratches with a gap distance >450 μm or <400 μm were excluded. 24 h after plates were scratched, phase contrast micrographs were taken using a Zeiss Axiovert A1 (Zeiss, Oberkochen, Germany), and the gap distance was measured using AxioVision 4.9 (Zeiss).

2.13. Cloning and purification of human c-subunit construct

The human ORF ATP-synthase c1 (ATP5G1) subunit construct (Origene Technologies), tagged on the C terminus with Myc and DDK (Flag), was overexpressed in XL-10 Gold-ultracompetent cells and DNA was isolated using the Qiagen plasmid maxi kit.

2.14. Overexpression of the F_1Fo ATP synthase c subunit

This procedure was performed as described previously [19,20]. Cells were transfected 24 h after seeding with 2 μg construct using the Lipofectamine LTX Reagent (Thermo Fisher Scientific, Waltham, MA). Cells were maintained by regular culture conditions for 48 h to allow for protein expression, and cells or cell lysates were treated as described in their respective figure legends.

2.15. Statistical analysis

Data are reported as the mean + SEM of at least three independent experiments. Difference in the means between 2 groups was tested using student's t-test. To compare 3 or more groups, one-way ANOVA with Tukey's post-hoc analysis was applied. $P < 0.05$ is considered statistically significant. P values are provided in figure legends.

3. Results

3.1. FSS increases proliferation of MCF7 and MDA-MB-231 breast cancer cells

MCF7 is an estrogen and progesterone receptor-expressing human breast cancer cell line that demonstrates lower metastatic potential in the absence of estrogen [21], whereas MDA-MB-231 is a triple-negative, metastatic breast cancer cell line that lacks receptors for estrogen, progesterone, and HER2. MCF7 and MDA-MB-231 breast cancer cells were treated with physiological levels of FSS, 0, 5, 20, and 60 dyn/cm^2. After FSS treatment, cells were re-seeded, mimicking CTC adhesion at the secondary location during metastasis. We monitored cell growth and counted cells 1, 2, 3, 5, and 7 days after seeding. There was no difference in cell proliferation between static and FSS-treated groups up to 3 days after cell seeding. However, after exposure to the higher levels of FSS (20 and 60 dyn/cm^2),

the number of MCF7 cells was increased at 7 days of incubation (Fig. 1A and B). The baseline growth rate of MDA-MB-231 cells was faster than MCF7 cells. FSS treatment significantly increased the proliferation of MDA-MB-231 breast cancer cells at 5 and 7 days of incubation (Fig. 1C and D), suggesting that FSS potentially influences the metastatic behavior of breast cancer.

3.2. FSS alters mitochondrial energy metabolism in breast cancer cells

Since cell division and growth require abundant ATP, we evaluated intracellular energy metabolism with and without FSS treatment. MCF7 and MDA-MB-231 cells were treated with FSS (60 dyn/cm^2) and seeded for 24 h. We first quantified the oxygen consumption rate by applying mitoXpress Xtra, a fluorescence probe quenched by oxygen. Treatment with FSS increased the oxygen consumption rates in both MCF7 (Fig. 2A) and MDA-MB-231 cells (Fig. 2B). Intracellular ATP was assayed by measuring luminescence generated by luciferase, luciferin, and ATP. Cell line differences in the proliferation data (Fig. 1) suggested that baseline ATP was higher in MDA-MB-231 cells than in MCF7 cells. Interestingly, FSS treatment resulted in additional ATP increases for MDA-MB-231 cells (Fig. 2C) but not MCF7 cells. Notably, FSS-treated breast cancer cells retained greater ATP after carbonyl cyanide 4-(trifluoromethoxy)phenylhydrazone (FCCP) challenge, indicating decreased reliance on mitochondrial energy metabolism. Moreover, MDA-MB-231 cells produced more lactate than MCF7 cells, and treatment with FSS increased lactate production in MCF7 cells, indicating enhanced aerobic glycolysis (Fig. 2D).

When measuring the mitochondrial inner membrane potential ($\Delta\psi$), we found the tetramethylrhodamine (TMRM) intensity in MDA-MB-231 cells was lower than in MCF7 cells, which further confirmed decreased reliance of MDA-MB-231 cells on oxidative phosphorylation (Fig. 2E and F). Moreover, treatment with oligomycin, a pharmacological inhibitor of F_1F_O ATP synthase, depolarized the mitochondrial inner membrane potential of MCF7 cells but not of MDA-MB-231 cells (Fig. 2G), which indicates that in these cells, the F_1F_O ATP synthase runs in a reverse ATP hydrolysis direction to energize the mitochondrial inner membrane. Therefore, F_1F_O ATP synthase inhibition by oligomycin depolarizes the inner membrane potential. The electron transport chain complexes I-IV are responsible for the generation of inner membrane potential during oxidative phosphorylation, which is then used by ATP synthase to synthesize ATP. Oligomycin inhibition should have induced the inner membrane hyperpolarization if F_1F_O ATP synthase was running in the ATP synthesis direction.

As aberrant functioning of the electron transport chain contributes to the generation of mitochondrial reactive oxygen species (ROS), we tested whether FSS changed intracellular redox status. We first measured endogenous hydrogen peroxide levels in MCF7 and MDA-MB-231 cells treated with or without FSS. Immediately after FSS treatment, the DCF fluorescence signal increased in both MCF7 (Fig. 2H) and MDA-MB-231 cells (Fig. 2I). FSS-treated cells maintained a greater DCF signal for 24 h, indicating the FSS-induced redox imbalance had a prolonged impact. When measuring the mitochondrial superoxide level using the mitoSOX fluorescent probe, we found that 24 h after FSS (60 dyn/cm^2)

treatment, both MCF7 (Fig. 2J) and MDA-MB-231 (Fig. 2K) cells increased mitoSOX fluorescence intensity.

3.3. FSS lowers protein levels of the F_1F_O ATP synthase c-subunit

Our team previously demonstrated that the c-subunit of F_1F_O ATP synthase forms the largest known candidate channel of mPTP, and depletion or blockage of the c-subunit improves mitochondrial energy metabolism and enhances cell survival and growth [11,22–25]. To test whether FSS-induced proliferative (Fig. 1) and anti-apoptotic characteristics [7] of breast cancer cells are associated with the c-subunit of F_1F_O ATP synthase, we quantified the expression of three genes that encode the c-subunit (*ATP5G1*, *ATP5G2*, and *ATP5G3*) 24 h after FSS exposure. We also quantified the expression of genes that encode the α-subunit (*ATP5A1* and *ATP5AF2*) and β-subunit (*ATP5B*, *ATPBL*, and *ATPAF*) of ATP synthase F_1 subcomplex which catalyzes ATP synthesis. We found that the three MCF7 c-subunit genes, *ATP5AF2* (α-subunit) and ATPAF (β-subunit), were decreased after FSS treatment (Fig. 3A–H). In MDA-MB-231 cells, expression of *ATP5G2, ATP5G3, ATP5AF2, ATP5B, ATPBL*, and *ATPAF* were significantly decreased, whereas *ATP5G1* and *ATP5A1* were increased (Fig. 3I–P). Furthermore, the protein levels of the c-subunit were significantly lower 24 h after FSS exposure (Fig. 3Q–T). The β-subunit protein, located in the F_1 complex that converts ADP to ATP, was also reduced.

3.4. Overexpression of F_1F_O ATP synthase c-subunit decreased proliferation of MCF7 breast cancer cells

To assess the importance of the c-subunit of F_1F_O ATP synthase in cancer cell proliferation, we overexpressed the c-subunit of F_1F_O ATP synthase in MCF7 and MDA-MB-231 breast cancer cells (Fig. 4A). MCF7 and MDA-MB-231 cells overexpressing the c-subunit were subjected to the scratch assay. Briefly, we drew a line on the plate and measured the gap distance 24 h after incubation. In the scratch assay, the gap distance in the MCF7 control and MDA-MB-231 control was 270 μm and 181 μm, respectively. However, c-subunit overexpression in the MCF7 and MDA-MB-231 experimental groups resulted in resistance to gap closure, and the gap distances were 437 μm and 319 μm, respectively (Fig. 4B and C). Our data indicate that c-subunit overexpression results in poor proliferative potential of MCF7 and MDA-MB-231 breast cancer cells.

4. Discussion

In this study, we found that FSS enhances the proliferation of MCF7 and MDA-MB-231 breast cancer cells by altering the abundance of the F_1F_O ATP synthase. Treatment with FSS decreases the F_1F_O ATP synthase c-subunit, impairing mitochondria-dependent cellular energy metabolism, whereas overexpression of the c-subunit arrests cancer cell proliferation in MCF7 and MDA-MB-231 cells.

The mPTP is a large unselective channel found in the mitochondrial inner membrane. Opening the mPTP causes the loss of mitochondrial membrane integrity and impairs cellular energy metabolism, ultimately leading to cell death. The F_1F_O ATP synthase is critical in governing cellular energy metabolism, because the F_1F_O ATP synthase phosphorylates ADP

to generate ATP and participates in mPTP formation. We have previously shown that the c-subunit contributes high aberrant mitochondrial channel conductance, whereas transduction with c-subunit shRNA protects cells from ROS or excitotoxicity-mediated death [11,15,16]. In this study, we found that treatment with FSS decreased c-subunit protein levels in MCF7 and MDA-MB-231 cells, indicating alteration of mitochondria-dependent cellular energy metabolism.

The impact of the c-subunit on cellular energy metabolism may differ in MCF7 and MDA-MB-231 cells. FSS-treated MCF7 cells demonstrated downregulation of genes encoding the c-subunit, including *ATP5G1, ATP5G2, ATP5G3*, and decreased c-subunit protein levels (Fig. 3). However, FSS did not change intracellular ATP levels (Fig. 2). Notably, when FSS-exposed MCF7 cells were challenged with FCCP, they were more resistant to FCCP-induced ATP depletion than static MCF7 cells. Therefore, FSS may trigger metabolic remodeling, increasing the cell's reliance on non-mitochondrial energy metabolism such as glycolysis. This proposed pathway is supported by our finding that treatment with FSS increased lactate production in MCF7 cells. Additionally, treatment with oligomycin decreased mitochondrial inner membrane potential in MCF7 cells, indicating inhibition of ATP hydrolysis.

In MDA-MB-231 cells, ATP levels in the static baseline were higher than in MCF7 cells, and treatment with FSS further increased ATP production. It is not surprising that MDA-MB-231 cells demonstrated higher lactate production than MCF7 cells since aerobic glycolysis is well characterized during metastasis. Static MDA-MB-231 cells maintained 52% intracellular ATP even after FCCP treatment; therefore, MDA-MB-231 cells may already rely heavily on aerobic glycolysis to maintain cellular energy metabolism. We also found that treatment with oligomycin was less effective on mitochondrial membrane potential in MDA-MB231 cells. Since MDA-MB-231 cells express a lower level of c-subunit protein than MCF7 cells, the impact of reversible F_1Fo ATP synthase activity may not be significant. It was unexpected to detect a lower TMRM signal in MDA-MB-231 cells. Based on our Western blot analysis, we speculate that the total number of mitochondria may differ between MCF7 and MDA-MB-231 cell lines. Future functional analysis of individual mitochondria may be informative.

We also found that FSS increased oxygen consumption of both MCF7 and MDA-MB-231 cells. Since FSS downregulates subunits of the F_1F_O ATP synthase and decreases oxidative phosphorylation, this finding was unexpected. We also found that breast cancer cells treated with FSS had increased ROS levels even after 24 h incubation. ROS play a dual role in regulating the death and survival of cancer cells. Surging ROS potentiates breast cancer cell death during treatment with chemotherapeutics such as cisplatin and doxorubicin [26,27], but moderate levels of ROS act as signaling molecules to upregulate survival proteins, supporting cancer cell growth [28–30]. Thus, our results are consistent with previous work that showed that elevated yet non-lethal ROS leads to cell proliferation [31], especially in cancer stem cell-like MDA-MB-231 cells. Although currently, there are limited approaches for manipulating c-subunit expression or activity in CTCs, our team and others have shown that the c-subunit is sensitive to oxidative stress, and depletion of the c-subunit is protective against hydrogen peroxide-mediated death in various cell models [11,13]. Additionally, the c-subunit undergoes conformational change between open and closed states. This change

means that the c-subunit can be dissociated from the F_1F_O ATP synthase complex, which may be controlled by intracellular redox status [11,15]. Although there has been less research on oxidative stress-induced post-translational modification of the c-subunit than the F_1 complex subunits [32,33], a cysteine residue found in the c-subunit undergoes thiol oxidation during oxidative stress, and this modification weakens the interaction between oligomycin and the c-subunit of the F_1F_O ATP synthase [34,35]. It is unknown if oxidation of a cysteine residue directly causes c-subunit opening. However, this study demonstrated that mitochondrial redox status might manipulate F_1F_O ATP synthase binding, potentially influencing the opening or closing of the c-subunit.

In contrast to our findings, researchers have previously elucidated the leak-dependent effect of electron transport [36,37]. They found that treatment with FCCP in the presence of oligomycin, an inhibitor of F_1F_O ATP synthase, increased the cell proliferation rate. These results suggest that reduced F_1F_O ATP synthase function with a greater leak is associated with higher cell proliferation [36,37]. Therefore, the c-subunit may exhibit a dual function: during moderate expression, the c-subunit may prevent hyperpolarization of the mitochondrial membrane, supporting intracellular energy metabolism, whereas overexpression of the c-subunit rapidly depolarizes mitochondria, impairs energy metabolism, and arrests cancer cell migration. Based on our Western blot data, cancer cells may maintain minimal levels of the c-subunit, supporting Warburg metabolism while protecting themselves from mPTP-mediated death. Future studies elucidating the ratio of the c-subunit to the mitochondrion or the whole cell may offer insight into the mechanisms of how cancer cells balance c-subunit levels to maintain metabolic benefits and avoid mPTP-associated death.

In summary, this study demonstrates that FSS promotes breast cancer cell proliferation via depletion of the c-subunit of F_1F_O ATP synthase. Overexpression of the c-subunit slowed the migration of MCF7 and MDA-MB-231 breast cancer cells. This study is the first to suggest the c-subunit as a target to manipulate the CTC survival rate. Investigating therapeutic strategies to upregulate the c-subunit may be beneficial in preventing metastasis via CTCs.

Acknowledgments

This work was supported by the University of Alabama's Alabama Life Research Institute ALRI-14565 (Y.K., and H.-A. P.), the U.S. Department of Education P200A180056 and P200A210069 (S.R.B.), and National Institute on Aging K01AG054734 and RF1AG072484 (N.M.).

References

[1]. Bidard FC, Peeters DJ, Fehm T, Nole F, Gisbert-Criado R, Mavroudis D, Grisanti S, Generali D, Garcia-Saenz JA, Stebbing J, Caldas C, Gazzaniga P, Manso L, Zamarchi R, de Lascoiti AF, De Mattos-Arruda L, Ignatiadis M, Lebofsky R, van Laere SJ, Meier-Stiegen F, Sandri MT, Vidal-Martinez J, Politaki E, Consoli F, Bottini A, Diaz-Rubio E, Krell J, Dawson SJ, Raimondi C, Rutten A, Janni W, Munzone E, Caranana V, Agelaki S, Almici C, Dirix L, Solomayer EF, Zorzino L, Johannes H, Reis-Filho JS, Pantel K, Pierga JY, Michiels S, Clinical validity of circulating tumour cells in patients with metastatic breast cancer: a pooled analysis of individual patient data, Lancet Oncol. 15 (2014) 406–414, 10.1016/S1470-2045(14)70069-5. [PubMed: 24636208]

[2]. Chaffer CL, Weinberg RA, A perspective on cancer cell metastasis, Science 331 (2011) 1559–1564, 10.1126/science.1203543. [PubMed: 21436443]

[3]. Cristofanilli M, Pierga JY, Reuben J, Rademaker A, Davis AA, Peeters DJ, Fehm T, Nole F, Gisbert-Criado R, Mavroudis D, Grisanti S, Giuliano M, Garcia-Saenz JA, Stebbing J, Caldas C, Gazzaniga P, Manso L, Zamarchi R, de Lascoiti AF, De Mattos-Arruda L, Ignatiadis M, Cabel L, van Laere SJ, Meier-Stiegen F, Sandri MT, Vidal-Martinez J, Politaki E, Consoli F, Generali D, Cappelletti MR, Diaz-Rubio E, Krell J, Dawson SJ, Raimondi C, Rutten A, Janni W, Munzone E, Caranana V, Agelaki S, Almici C, Dirix L, Solomayer EF, Zorzino L, Darrigues L, Reis-Filho JS, Gerratana L, Michiels S, Bidard FC, Pantel K, The clinical use of circulating tumor cells (CTCs) enumeration for staging of metastatic breast cancer (MBC): international expert consensus paper, Crit. Rev. Oncol. Hematol. 134 (2019) 39–45, 10.1016/j.critrevonc.2018.12.004. [PubMed: 30771872]

[4]. Riebensahm C, Joosse SA, Mohme M, Hanssen A, Matschke J, Goy Y, Witzel I, Lamszus K, Kropidlowski J, Petersen C, Kolb-Kokocinski A, Sauer S, Borgmann K, Glatzel M, Muller V, Westphal M, Riethdorf S, Pantel K, Wikman H, Clonality of circulating tumor cells in breast cancer brain metastasis patients, Breast Cancer Res. 21 (2019) 101, 10.1186/s13058-019-1184-2. [PubMed: 31481116]

[5]. Sparano J, O'Neill A, Alpaugh K, Wolff AC, Northfelt DW, Dang CT, Sledge GW, Miller KD, Association of circulating tumor cells with late recurrence of estrogen receptor-positive breast cancer: a secondary analysis of a randomized clinical trial, JAMA Oncol. 4 (2018) 1700–1706, 10.1001/jamaoncol.2018.2574. [PubMed: 30054636]

[6]. Franken B, de Groot MR, Mastboom WJ, Vermes I, van der Palen J, Tibbe AG, Terstappen LW, Circulating tumor cells, disease recurrence and survival in newly diagnosed breast cancer, Breast Cancer Res. 14 (2012) R133, 10.1186/bcr3333. [PubMed: 23088337]

[7]. Triantafillu U, Park S, Kim Y, Fluid shear stress induces drug resistance to doxorubicin and paclitaxel in the breast cancer cell line MCF7, Advanced Therapeutics 2 (2019), 1800112, 10.1002/adtp.201800112.

[8]. Agnoletto C, Corra F, Minotti L, Baldassari F, Crudele F, Cook WJJ, Di Leva G, d'Adamo AP, Gasparini P, Volinia S, Heterogeneity in circulating tumor cells: the relevance of the stem-cell subset, Cancers 11 (2019), 10.3390/cancers11040483.

[9]. Triantafillu UL, Park S, Klaassen NL, Raddatz AD, Kim Y, Fluid shear stress induces cancer stem cell-like phenotype in MCF7 breast cancer cell line without inducing epithelial to mesenchymal transition, Int. J. Oncol. 50 (2017) 993–1001, 10.3892/ijo.2017.3865. [PubMed: 28197635]

[10]. Mnatsakanyan N, Llaguno MC, Yang Y, Yan Y, Weber J, Sigworth FJ, Jonas EA, A mitochondrial megachannel resides in monomeric F1FO ATP synthase, Nat. Commun. 10 (2019) 5823, 10.1038/s41467-019-13766-2. [PubMed: 31862883]

[11]. Alavian KN, Beutner G, Lazrove E, Sacchetti S, Park HA, Licznerski P, Li H, Nabili P, Hockensmith K, Graham M, Porter GA Jr., Jonas EA, An uncoupling channel within the c-subunit ring of the F1FO ATP synthase is the mitochondrial permeability transition pore, Proc. Natl. Acad. Sci. U. S. A. 111 (2014) 10580–10585, 10.1073/pnas.1401591111. [PubMed: 24979777]

[12]. Neginskaya MA, Solesio ME, Berezhnaya EV, Amodeo GF, Mnatsakanyan N, Jonas EA, Pavlov EV, ATP synthase C-Subunit-Deficient mitochondria have a small cyclosporine A-sensitive channel, but lack the permeability transition pore, Cell Rep. 26 (2019) 11–17, 10.1016/j.celrep.2018.12.033, e12. [PubMed: 30605668]

[13]. Bonora M, Bononi A, De Marchi E, Giorgi C, Lebiedzinska M, Marchi S, Patergnani S, Rimessi A, Suski JM, Wojtala A, Wieckowski MR, Kroemer G, Galluzzi L, Pinton P, Role of the c subunit of the FO ATP synthase in mitochondrial permeability transition, Cell Cycle 12 (2013) 674–683, 10.4161/cc.23599. [PubMed: 23343770]

[14]. Azarashvili T, Odinokova I, Bakunts A, Ternovsky V, Krestinina O, Tyynela J, Saris NE, Potential role of subunit c of F0F1-ATPase and subunit c of storage body in the mitochondrial permeability transition. Effect of the phosphorylation status of subunit c on pore opening, Cell Calcium 55 (2014) 69–77, 10.1016/j.ceca.2013.12.002. [PubMed: 24380588]

[15]. Mnatsakanyan N, Park HA, Wu J, He X, Llaguno MC, Latta M, Miranda P, Murtishi B, Graham M, Weber J, Levy RJ, Pavlov EV, Jonas EA, Mitochondrial ATP synthase c-subunit leak

channel triggers cell death upon loss of its F1 subcomplex, Cell Death Differ. (2022), 10.1038/s41418-022-00972-7.

[16]. Park HA, Licznerski P, Mnatsakanyan N, Niu Y, Sacchetti S, Wu J, Polster BM, Alavian KN, Jonas EA, Inhibition of Bcl-xL prevents pro-death actions of DeltaN-Bcl-xL at the mitochondrial inner membrane during glutamate excitotoxicity, Cell Death Differ. 24 (2017) 1963–1974, 10.1038/cdd.2017.123. [PubMed: 28777375]

[17]. Duan Y, Gross RA, Sheu SS, Ca2+-dependent generation of mitochondrial reactive oxygen species serves as a signal for poly(ADP-ribose) polymerase-1 activation during glutamate excitotoxicity, J. Physiol. 585 (2007) 741–758, 10.1113/jphysiol.2007.145409. [PubMed: 17947304]

[18]. Park HA, Mnatsakanyan N, Broman K, Davis AU, May J, Licznerski P, Crowe-White KM, Lackey KH, Jonas EA, Alpha-Tocotrienol prevents oxidative stress-mediated post-translational cleavage of bcl-xL in primary hippocampal neurons, Int. J. Mol. Sci. 21 (2019), 10.3390/ijms21010220.

[19]. Park HA, Khanna S, Rink C, Gnyawali S, Roy S, Sen CK, Glutathione disulfide induces neural cell death via a 12-lipoxygenase pathway, Cell Death Differ. 16 (2009) 1167–1179, 10.1038/cdd.2009.37. [PubMed: 19373248]

[20]. Park HA, Kubicki N, Gnyawali S, Chan YC, Roy S, Khanna S, Sen CK, Natural vitamin E alpha-tocotrienol protects against ischemic stroke by induction of multidrug resistance-associated protein 1, Stroke 42 (2011) 2308–2314, 10.1161/STROKEAHA.110.608547. [PubMed: 21719775]

[21]. Comsa S, Cimpean AM, Raica M, The story of MCF-7 breast cancer cell line: 40 years of experience in research, Anticancer Res. 35 (2015) 3147–3154. [PubMed: 26026074]

[22]. Alavian KN, Li H, Collis L, Bonanni L, Zeng L, Sacchetti S, Lazrove E, Nabili P, Flaherty B, Graham M, Chen Y, Messerli SM, Mariggio MA, Rahner C, McNay E, Shore GC, Smith PJ, Hardwick JM, Jonas EA, Bcl-xL regulates metabolic efficiency of neurons through interaction with the mitochondrial F1FO ATP synthase, Nat. Cell Biol. 13 (2011) 1224–1233, 10.1038/ncb2330. [PubMed: 21926988]

[23]. Bonora M, Pinton P, Shedding light on molecular mechanisms and identity of mPTP, Mitochondrion 21 (2015) 11, 10.1016/j.mito.2014.10.001. [PubMed: 25315653]

[24]. Bonora M, Wieckowski MR, Chinopoulos C, Kepp O, Kroemer G, Galluzzi L, Pinton P, Molecular mechanisms of cell death: central implication of ATP synthase in mitochondrial permeability transition, Oncogene 34 (2015) 1475–1486, 10.1038/onc.2014.96. [PubMed: 24727893]

[25]. Chen R, Park HA, Mnatsakanyan N, Niu Y, Licznerski P, Wu J, Miranda P, Graham M, Tang J, Boon AJW, Cossu G, Mandemakers W, Bonifati V, Smith PJS, Alavian KN, Jonas EA, Parkinson's disease protein DJ-1 regulates ATP synthase protein components to increase neuronal process outgrowth, Cell Death Dis. 10 (2019) 469, 10.1038/s41419-019-1679-x. [PubMed: 31197129]

[26]. Marullo R, Werner E, Degtyareva N, Moore B, Altavilla G, Ramalingam SS, Doetsch PW, Cisplatin induces a mitochondrial-ROS response that contributes to cytotoxicity depending on mitochondrial redox status and bioenergetic functions, PLoS One 8 (2013), e81162, 10.1371/journal.pone.0081162. [PubMed: 24260552]

[27]. Pilco-Ferreto N, Calaf GM, Influence of doxorubicin on apoptosis and oxidative stress in breast cancer cell lines, Int. J. Oncol. 49 (2016) 753–762, 10.3892/ijo.2016.3558. [PubMed: 27278553]

[28]. Chen N, Chen X, Huang R, Zeng H, Gong J, Meng W, Lu Y, Zhao F, Wang L, Zhou Q, BCL-xL is a target gene regulated by hypoxia-inducible factor-1 {alpha, J. Biol. Chem. 284 (2009) 10004–10012, 10.1074/jbc.M805997200. [PubMed: 19211554]

[29]. Chen C, Edelstein LC, Gelinas C, The Rel/NF-kappaB family directly activates expression of the apoptosis inhibitor Bcl-x(L), Mol. Cell Biol. 20 (2000) 2687–2695. [PubMed: 10733571]

[30]. Niture SK, Jaiswal AK, Nrf2-induced antiapoptotic Bcl-xL protein enhances cell survival and drug resistance, Free Radic. Biol. Med. 57 (2013) 119–131, 10.1016/j.freeradbiomed.2012.12.014. [PubMed: 23275004]

[31]. Tuy K, Rickenbacker L, Hjelmeland AB, Reactive oxygen species produced by altered tumor metabolism impacts cancer stem cell maintenance, Redox Biol. 44 (2021), 101953, 10.1016/j.redox.2021.101953. [PubMed: 34052208]

[32]. Kaludercic N, Giorgio V, The dual function of reactive oxygen/nitrogen species in bioenergetics and cell death: the role of ATP synthase, Oxid. Med. Cell. Longev. (2016), 3869610, 10.1155/2016/3869610, 2016. [PubMed: 27034734]

[33]. Wang SB, Murray CI, Chung HS, Van Eyk JE, Redox regulation of mitochondrial ATP synthase, Trends Cardiovasc. Med. 23 (2013) 14–18, 10.1016/j.tcm.2012.08.005. [PubMed: 23312134]

[34]. Nesci S, Ventrella V, Trombetti F, Pirini M, Pagliarani A, Thiol oxidation is crucial in the desensitization of the mitochondrial F1FO-ATPase to oligomycin and other macrolide antibiotics, Biochim. Biophys. Acta 1840 (2014) 1882–1891, 10.1016/j.bbagen.2014.01.008. [PubMed: 24412197]

[35]. Symersky J, Osowski D, Walters DE, Mueller DM, Oligomycin frames a common drug-binding site in the ATP synthase, Proc. Natl. Acad. Sci. U. S. A. 109 (2012) 13961–13965, 10.1073/pnas.1207912109. [PubMed: 22869738]

[36]. Luengo A, Li Z, Gui DY, Sullivan LB, Zagorulya M, Do BT, Ferreira R, Naamati A, Ali A, Lewis CA, Thomas CJ, Spranger S, Matheson NJ, Vander Heiden MG, Increased demand for NAD(+) relative to ATP drives aerobic glycolysis, Mol. Cell 81 (2021) 691e707, 10.1016/j.molcel.2020.12.012, e696. [PubMed: 33382985]

[37]. Sullivan LB, Gui DY, Hosios AM, Bush LN, Freinkman E, Vander Heiden MG, Supporting aspartate biosynthesis is an essential function of respiration in proliferating cells, Cell 162 (2015) 552–563, 10.1016/j.cell.2015.07.017. [PubMed: 26232225]

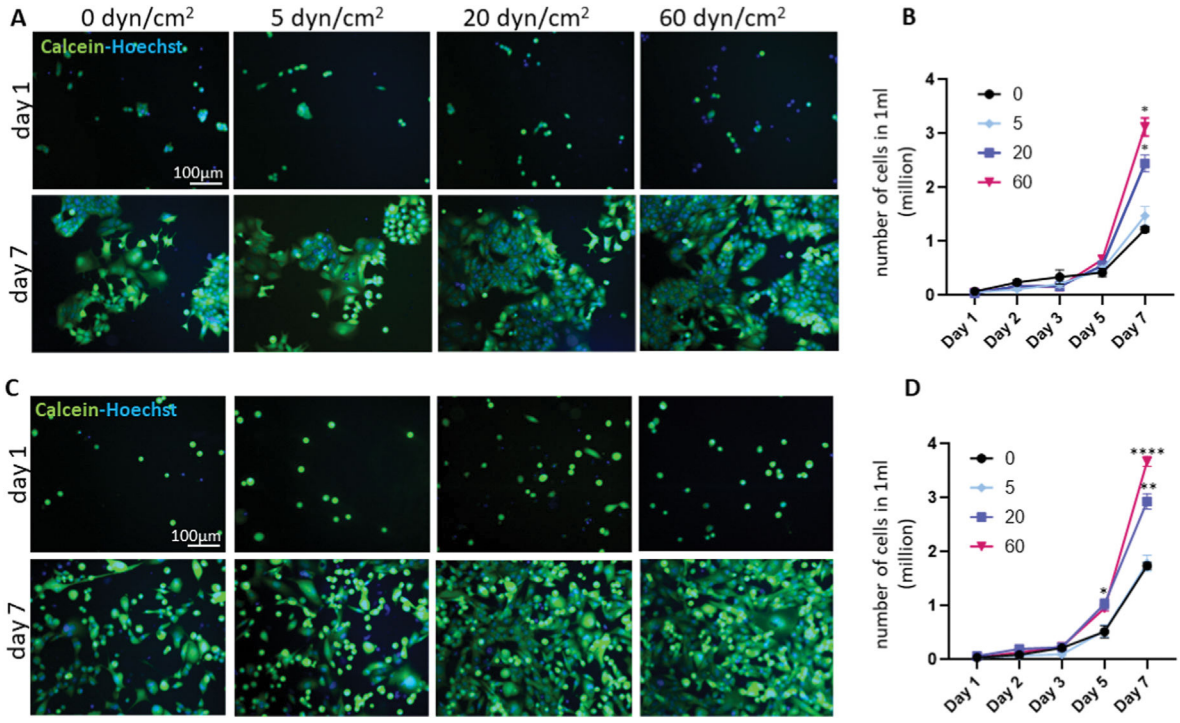

Fig. 1.

FSS increases the proliferation of breast cancer cells.

MCF7 (**A–B**) or MDA-MB-231 (**C-D**) breast cancer cells were treated with 0, 5, 20, and 60 dyn/cm^2 FSS and cells were counted 1, 2, 3, 5 and 7 days after seeding. Calcein and Hoechst were used to visualize viable cells and nuclei, respectively. FSS (20 and 60 dyn/cm^2) increased proliferation of both cell types (n = 3). Green: Calcein; Blue: Hoechst. *p < 0.05, **p < 0.01, ***p < 0.001, and ****p < 0.0001, one-way ANOVA with Tukey post hoc analysis.

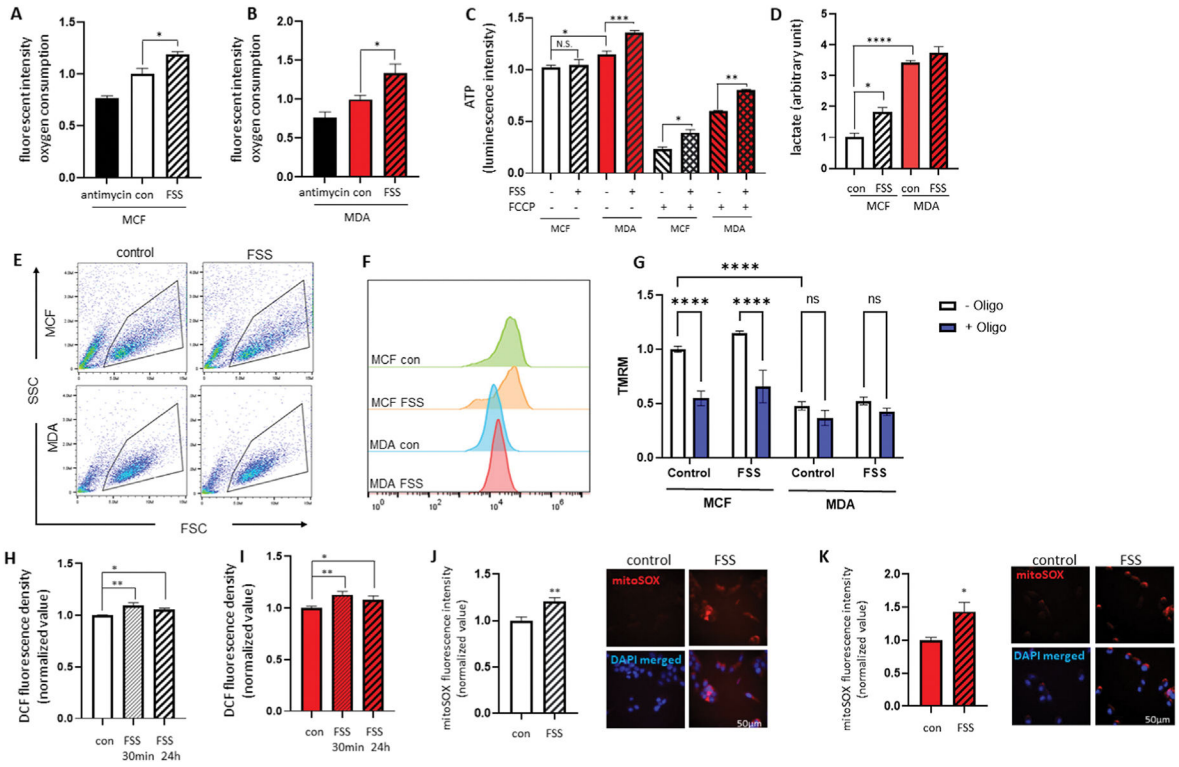

Fig. 2.

FSS alters the cellular energy metabolism of breast cancer cells.

MCF7 and MDA-MB-231 cells were treated with or without FSS (60 dyn/cm^2) and seeded for 24 h. FSS enhanced the MitoXpress Xtra signal in both MCF7 (**A**) and MDA-MB-231 cells (**B**), indicating an increased cellular oxygen consumption rate (n = 4). (**C**) MCF7 and MDA-MB-231 cells treated with FSS were resistant to ATP loss during FCCP treatment (n = 4). (**D**) MDA-MB-231 cells generated a higher lactate level than MCF7 cells, and FSS treatment increased lactate production in MCF7 cells (n = 3). Representative flow cytometry dot plots (**E**), histograms (**F**), and group data (**G**) show TMRM intensity in MCF7 and MDA-MB-231 cells (n = 3). MCF7 (**H**) and MDA-MB-231 (**I**) cells were treated with or without FSS (60 dyn/cm^2) and seeded for 30 min and 24 h. Intracellular hydrogen peroxide levels were assayed by measuring 2′, 7′-dichlorofluorescein (DCF). Breast cancer cells treated with FSS demonstrated increased DCF signals (n = 3). MCF7 (**J**) and MDA-MB-231 (**K**) cells were treated with or without FSS (60 dyn/cm2) and seeded for 24 h, and the mitochondrial superoxide level was measured using mitoSOX. Treatment with FSS increased the mitoSOX signal in MCF7 (n = 4) and MDA-MB-231 (n = 6) cells. *p < 0.05, **p < 0.01, ***p < 0.001, and ****p < 0.0001, one-way ANOVA with Tukey post hoc analysis.

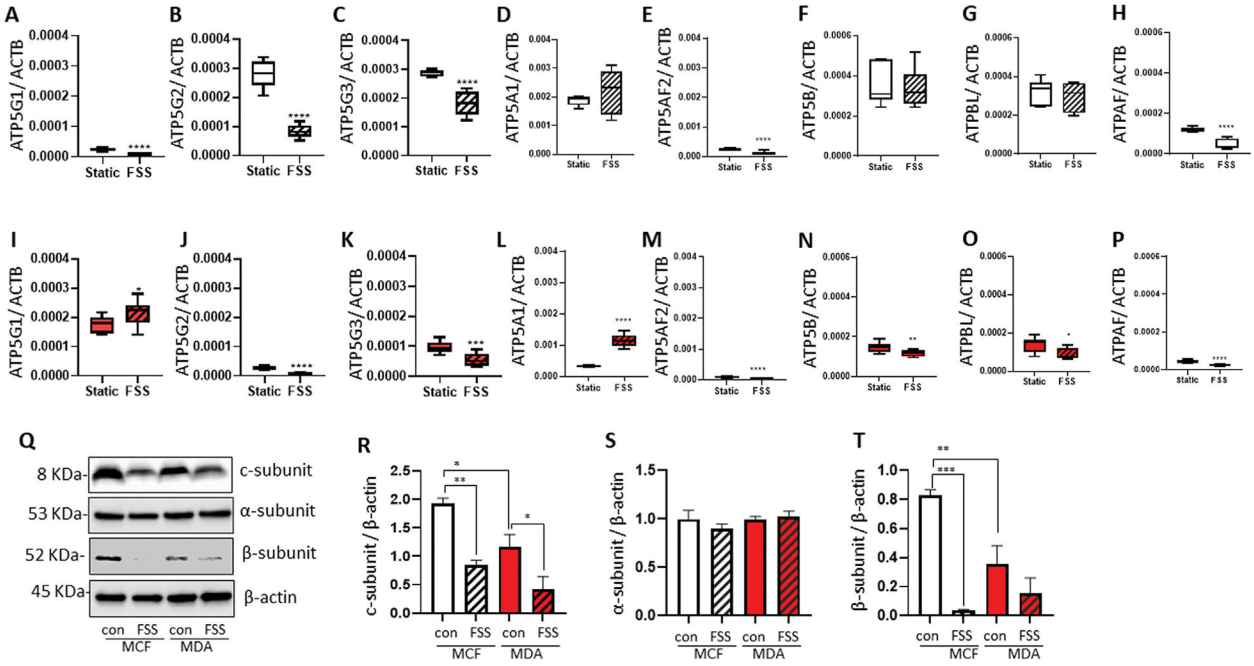

Fig. 3.

FSS alters the expression of the F1FO ATP synthase subunits.

MCF7 and MDA-MB-231 cells were treated with or without FSS (60 dyn/cm^2) and seeded for 24 h. The mRNA levels of genes that encode the c-subunit (**A-C**), α-subunit (**D-E**), and β-subunit (**F–H**) in MCF7 cells, and c-subunit (**I–K**), α-subunit (**L-M**), and β-subunit (**N–P**) in MDA-MB-231 cells were quantified (n = 9). **Q-T**, Immunoblot data demonstrated that FSS did not change the α-subunit (**S**, n = 4) but decreased protein levels of the c-subunit (**R**, n = 4) and β-subunit (**T**, n = 3). *p < 0.05, **p < 0.01, ***p < 0.001, and ****p < 0.0001, one-way ANOVA with Tukey post hoc analysis.

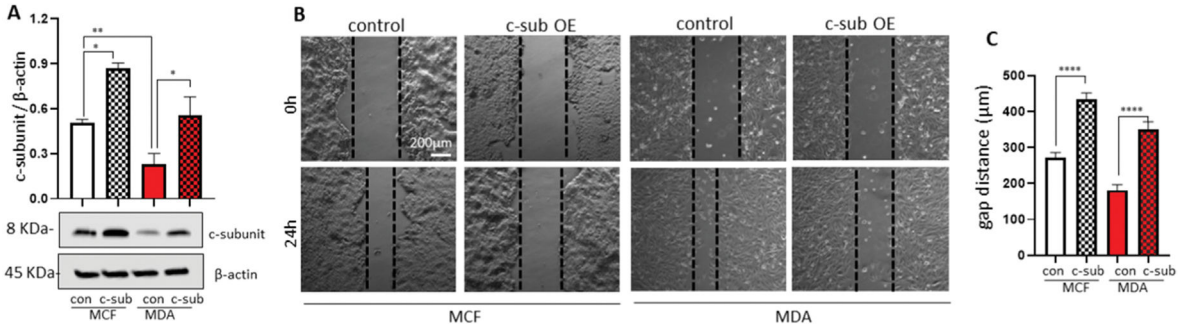

Fig. 4.

Overexpression of the F1FO ATP synthase c-subunit decreases the proliferation of breast cancer cells.

The c-subunits were overexpressed in MCF7 and MDA-MB-231 breast cancer cells. Immunoblot data verified overexpression of the c-subunit (**A**, n = 4). (**B**) c-subunit overexpressing MCF7 cells were re-seeded at high density (0.8 × 106 cells/35 mm plate). Micrographs were taken immediately after scratching plates and 24 h after incubation of MCF7 and MDA-MB-231 cells. (**C**) Gap distance after 24 h (n = 12). Scale bar = 200 μm **p < 0.05, **p < 0.01, ***p < 0.001, and ****p < 0.0001, one-way ANOVA with Tukey post hoc analysis.